



Silicone - barium titanate composites with increased electromechanical sensitivity. The effects of the filler morphology

Journal:	<i>RSC Advances</i>
Manuscript ID:	RA-ART-09-2014-009903.R1
Article Type:	Paper
Date Submitted by the Author:	n/a
Complete List of Authors:	Bele, Adrian; "Petru Poni" Institute of Macromolecular Chemistry, Cazacu, Maria; "Petru Poni" Institute of Macromolecular Chemistry, Inorganic Polymers Stiubianu, George Theodor; "Petru Poni" Institute of Macromolecular Chemistry, Vlad, Stelian; "Petru Poni" Institute of Macromolecular Chemistry,

RSC Advances

An international journal to further the chemical sciences



RSC Advances is an international, peer-reviewed, online journal covering all of the chemical sciences, including interdisciplinary fields.

The **criteria for publication** are that the experimental and/ or theoretical work must be **high quality, well conducted** and **demonstrate an advance by adding to the development of the field**.

RSC Advances 2013 Impact Factor* = 3.7

Thank you for your assistance in evaluating this manuscript.

Guidelines to the referees

Referees have the responsibility to treat the manuscript as confidential. Please be aware of our [Ethical Guidelines](#), which contain full information on the responsibilities of referees and authors, and our [Refereeing Procedure and Policy](#).

It is essential that all research work reported in RSC Advances is well-carried out and well-characterised. There should be enough supporting evidence for the claims made in the manuscript.

When preparing your report, please:

- comment on the originality and scientific reliability of the work;
- comment on the characterisation of the compounds/materials reported - has this been accurately interpreted and does it support the conclusions of the work;
- state clearly whether you would like to see the article accepted or rejected and give detailed comments (with references, as appropriate) that will both help the Editor to make a decision on the article and the authors to improve it.

Please inform the Editor if:

- there is a conflict of interest
- there is a significant part of the work which you are not able to referee with confidence
- the work, or a significant part of the work, has previously been published
- you believe the work, or a significant part of the work, is currently submitted elsewhere
- the work represents part of an unduly fragmented investigation.

For further information about RSC Advances, please visit: www.rsc.org/advances or contact us by email: advances@rsc.org.

*Data based on 2013 Journal Citation Reports®, (Thomson Reuters, 2014).

ARTICLE

Silicone - barium titanate composites with increased electromechanical sensitivity. The effects of the filler morphology

Cite this: DOI: 10.1039/x0xx00000x

A. Bele,^a M. Cazacu,^{a*} G. T. Stiubianu^a and S. Vlad^a

Received 00th September 2014,
Accepted 00th xxxxxx

DOI: 10.1039/x0xx00000x

www.rsc.org/

High molecular weight polydimethylsiloxane- α,ω -diol, synthesized in lab, was used as matrix for nanocomposites. Barium titanate as nanoparticles either cubic or nanorods were obtained by hydrothermal procedure and used as filler. In order to assure a good compatibility with the matrix, the filler was surface treated with a commercial surfactant. A highly reactive trifunctional silane was used as crosslinking agent in presence of organometallic catalyst. Two other samples, the first consisting in pure crosslinked polydimethylsiloxane and the second being the polymer matrix filled with commercial barium titanate, were prepared and used as reference to evaluate the influence of barium titanate nanoparticles presence and of their shape on some characteristics of the resulted crosslinked composites: morphology, thermal behavior, moisture sorption, mechanical and dielectric characteristics. The electromechanical sensitivity and energy output were calculated on the basis of the proper experimental data in order to estimate the potential of the composites for future electromechanical applications.

Introduction

There is a growing interest for materials with high electromechanical sensitivity, because such materials are useful as capacitors that can store large amount of energy and then deliver it instantaneously,¹⁻⁴ as novel potential electromechanical actuators that deform when stimulated by an electrical field,⁵⁻⁷ or as sensors used mainly for damage detection, characterization of structures and fatigue studies of materials.^{5,8} Therefore, many studies have been carried out to develop high permittivity materials¹. Polymeric materials having large dielectric constant and high energy density are promising for electromechanical energy conversion technologies.^{3,4,9} Besides fluoropolymers, acrylic polymers, polyurethanes and other synthetic or natural rubbers, silicones are often chosen for such purpose. Due to their structural peculiarities (high flexibility of the Si-O bond, low intermolecular interactions), silicones, with polydimethylsiloxane (PDMS) as the main representative of this type of polymers, have high free volume, low glass transition temperature and unusual rheological/flow properties with highly elastic behaviour.^{10,11} The polarizability of the Si-O bond, a premise for a high dielectric constant, is larger when compared to organic nonpolar polymers (e.g., polyethylene), but not as much as the theoretical values because the side organic groups (methyl groups in the case of PDMS) hinder the dipoles in getting too close to each other.^{12,13} In order to increase the dielectric constant the polysiloxanes are chemically modified by attaching polar groups to the silicon atoms.¹⁴⁻¹⁶ Although this procedure proved to be an efficient pathway, due to incompatibility between dimethylsiloxane segments of the main chain and polar groups it has the disadvantage that with increasing content of such groups phase separation phenomenon appears, thus leading to worsening of the mechanical properties of the resulted material.^{16,17}

Another approach consists in the incorporation of highly dielectric or conductive nanofillers in polymeric matrix to obtain high permittivity nanocomposites which combine the useful properties of polymers, such as versatile chemistry, flexibility, light weight and processability, with the superior electrical properties of adequate nanofiller.^{3,18} High-performance dielectric materials such as ferroelectric ceramic particles are often used in this aim because of their high dielectric constant and low dielectric loss^{1,19,20} but used alone such materials show the disadvantages of limited tunability of their own dielectric properties, high production cost and poor processability.¹⁸ A well-known ceramic is BaTiO₃, which is in the tetragonal phase in the temperature range between 5 and 120 °C, and in this phase it is a ferroelectric crystalline material exhibiting spontaneous polarization, with the dipole moment arising mainly because of the movement of Ti atoms with respect to the O atoms in the same plane inside the O₆ octahedra.²¹ It has been proved that particles of BaTiO₃ suspended in a medium show dielectric relaxation, similar to that observed for polar molecules and the dielectric behaviour is influenced by the size and structure of the aggregates.¹ Thus, the capacity of spherical particles to increase the dielectric constant is small at low volume fractions.²² Higher volume fractions lead to increased dielectric constant, but also to a reduction in electrical breakdown strength and mechanical properties.^{1,23-26} The particles in a colloidal suspension subjected to a strong electric field are polarized and tend to form chainlike aggregates oriented in the direction of electric field,²⁷⁻³⁰ this behavior being known as the Winslow effect.^{27,28} This effect is more pronounced when high aspect ratio fillers are used, this being a promising path for the development of materials with high dielectric constant and low dielectric loss at a low filler volume fraction, for use as capacitor and electric field materials.¹

In this work, we used barium titanate particles with prismatic and nanorod shapes, prepared by hydrothermal procedure, as a filler for a well-defined, high molecular weight polydimethylsiloxane- α,ω -diol ($M_n = 438\,000$) crosslinked with methyltriacetoxysilane in presence of dibutyltindilaurate as catalyst. We have chosen barium titanate due to its high dielectric permittivity, $\epsilon' \sim 1600$ at room temperature. In addition, the approached hydrothermal preparation method is simple, reproducible and easily scalable one. Because the dielectric permittivity depends on many factors, such as the grain size, shape and size of the crystals, impurities, and on processing techniques,³¹ here we studied the effect of its morphology. One sample, a pure crosslinked polymer and one consisting of polymer filled with commercial barium titanate were prepared and used as reference to evaluate the influence of the barium titanate presence and its morphology on some characteristics (dispersability, thermal and moisture sorption) of the resulted materials and properties of interest for electromechanical applications (dielectric and mechanical parameters). The presumptive electromechanical sensitivity was estimated on the basis of mechanical and dielectric measurements.

Experimental

Materials

The polydimethylsiloxane- α,ω -diol, that was used as matrix, was prepared by bulk polymerization of octamethylcyclotetrasiloxane catalyzed by H_2SO_4 , at room temperature and atmospheric humidity, according to an already described procedure.³² The average molecular mass values of the polymer, as estimated from the monomodal elution curve traced by gel permeation chromatography, with $CHCl_3$ as eluent, after calibration with standard polystyrene samples, were $M_n=438\,000$ and $M_w=641\,000$ (polydispersity index, $I=1.46$).

Barium titanate, $BaTiO_3$, BT, coded as CO to indicate filler type, with particle size $<3\ \mu m$ and PLURONIC L-31, HO-poly(ethyleneglycol)-*block*-poly(propyleneglycol)-*block*-poly(ethyleneglycol)-OH ($M=1100$, $d_{25}^{25} = 1.02$) were purchased from Fluka AG, barium chloride dihydrate, $BaCl_2 \cdot 2H_2O$ from Chimopar S.A. Romania, and titanium dioxide, Ti-Pure[®] R-902+ (min. 93 wt% TiO_2 , a rutile titanium dioxide pigment as a fine, dry powder) from Du Pont USA.

Methyltriacetoxysilane (MTAS) has been prepared by a procedure adapted from the literature³³ that consists in a simple condensation reaction between methyltrichlorosilane and acetic anhydride in stoichiometric ratio (1:3). Acetic anhydride was dropwise added over methyltrichlorosilane under stirring at room temperature, after that a condenser was attached to the reaction vessel and the temperature of the reaction mixture was increased to $110\ ^\circ C$ in order to remove acetyl chloride (vapour temperature $53\ ^\circ C$), a byproduct of the condensation reaction. Finally a vacuum of 10 mm Hg was applied to collect methyltriacetoxysilane (yield around 75%, b.p.₁₀ = $95-97\ ^\circ C$, $d_{20}^{20} = 1.17$, freezing point $\sim 40\ ^\circ C$).

Equipments

Scanning electron microscopy (SEM) images were acquired with an electronic microscope type Quanta 200 operating at 30 kV with secondary and backscattering electrons in low or high vacuum mode.

Transmission electron microscopy (TEM) observations were made with Hitachi High-Tech HT7700 Transmission Electron Microscope, operated in high contrast mode at 100 kV accelerating voltage. The samples were prepared on carbon coated copper grids of 300 mesh size. Microdrops of dispersions previously ultrasonicated in

chloroform were placed on the grids, and then solvent was removed in vacuum. A vacuum of $>10^{-4}$ torr was achieved in the sample holder room before performing the analysis.

Wide Angle X-rays Diffraction (WAXD) measurements were performed on a Bruker-AXS D8 ADVANCE diffractometer, with Bragg Brentano parafocusing goniometer and Cu anode with $\lambda = 1.5406$.

Stress-strain measurements were performed on TIRA test 2161 apparatus, Maschinenbau GmbH Ravenstein, Germany on dumbbell-shaped cut samples with dimensions of $50 \times 8.5 \times 4\ mm$. Measurements were run at an extension rate of 20 mm/min, at room temperature. Cyclic tensile stress tests were performed on the similar samples between 2 and 100 % strain. Five stretch-recovery cycles were registered. The stationary time at minimum and maximum applied stress was 5 s.

Dielectric spectroscopy was performed using the Novocontrol "Concept 40" broadband dielectric spectrometer (Hundsangen, Germany), at room temperature in the frequency domain 1 Hz–1 MHz. Samples in the form of films having uniform thickness in the 0.7-1 mm range were placed between gold plated round electrodes, the upper electrode having a 20 mm diameter. Temperature was controlled using a nitrogen gas cryostat and the temperature stability of the sample was better than $0.1\ ^\circ C$.

Water vapor sorption (DVS) capacity of the samples was determined in dynamic regime, in the relative humidity (RH) range 0–90 % by using the fully automated gravimetric analyzer IGAsorp produced by Hiden Analytical, Warrington (UK).

Dielectric strength measurements were made at PERCRO Laboratory - TeCIP Institute - Scuola Superiore Sant'Anna, Pisa, Italy, on a home-made installation consisting in high-speed high-voltage power amplifier, function generator, and an oscilloscope. The brass electrodes were applied on the film samples and the measurements were performed at 60 Hz, and a voltage increase rate of 2000 V/s at room temperature ($25\ ^\circ C$). The samples were previously brought into equilibrium with the humidity of the environment in which the measurements were made. Three samples were analyzed for each composite formulation and the lowest value was taken into consideration.

Thermogravimetric (TG) measurements were conducted on a STA 449 F1 Jupiter device (Netzsch, Germany), in nitrogen atmosphere, in the temperature range $25\ ^\circ C - 700\ ^\circ C$ at a heating rate of $10\ ^\circ C\ min^{-1}$. DSC measurements were conducted with a DSC 200 F3 Maia (Netzsch, Germany) at a heating rate of $10\ ^\circ C \cdot min^{-1}$ in nitrogen atmosphere.

Procedure

Preparation of barium titanate with different morphologies, CU and NR

In order to synthesize cubic barium titanate (CU) proper amounts of TiO_2 (0.25 g) and $BaCl_2$ (0.65 g) were mixed together in 20 mL of 10M NaOH aqueous solution.³⁴ The same amounts of TiO_2 and $BaCl_2$ were used to synthesize barium titanate nanorods (NR) in 20 mL of 5M NaOH aqueous solution. The resulting mixtures were transferred in stainless steel autoclaves coated with Teflon and kept 72 h at $200\ ^\circ C$ in a Venticell 55 hydrothermal oven. Heating and cooling of samples were done with a rate of $1\ ^\circ C/min$. After cooling, the particles were washed with distilled water by centrifugation at 6000 rpm for 15 min. This was repeated for 2 more times. Then the

particles were heated at 100°C over night in a laboratory oven to remove the remaining water before analyses.

Preparation of the silicone nanocomposites, C-CO, C-CU, C-NR, C-R

0.5 g barium titanate, either commercial (CO) or obtained as in the above described procedure (CU or NR), was grounded using an agate mortar with pestle and then was mixed with 0.5 g surfactant by vigorous mechanical stirring followed by ultrasonication for 5 minutes. The mixture was then transferred over 10 g PDMS and stirred again. Then 0.25 ml crosslinker (MTAS) and 0.025 mL catalyst (DBTDL) were added and stirred thoroughly until the components formed a homogenous mixture. The resulted mixture was sonicated for 10 minutes and afterwards it was poured into a Teflon mold (15x5 cm). The molds were maintained in atmospheric humidity at room temperature for 24 h so that crosslinking of the silicone matrix could occur. After that the formed films with thickness between 0.5 and 0.7 mm were easily peeled off from the substrate. The films labeled as C-CO (polymer matrix with commercial barium titanate as filler), C-CU (polymer matrix with cubic barium titanate nanoparticles as filler) and C-NR (polymer matrix with barium titanate nanorods as filler). A similar film consisting in pure crosslinked PDMS without any filler has been prepared as a reference sample, C-R. The films were then kept in the laboratory environment about two weeks for aging before characterization by different techniques (DSC, TGA, dielectric measurements and mechanical testing).

Results and discussions

A poly(dimethylsiloxane)- α,ω -diol of high molecular mass was prepared by a known procedure (bulk cationic ring-opening polymerization at room temperature) and used as matrix for a ceramic filler, i.e., barium titanate to obtain films with increased electromechanical sensitivity. Barium titanate particles with cubic (CU) and nanorod (NR) morphologies were prepared in this aim by hydrothermal technique. The cubes were obtained with dimensions ranging from 350 nm up to 550 nm on each side, while the nanorods had about 200 nm in diameter and 2-3 μm in length as could be estimated based on scanning and transmission electron microscopy images (Figure 1b,c,e,f). For commercial product, although SEM images taken on powder spread as such onto a substrate indicate large prisms with high dispersity in size (between 1-7 μm) (Figure 1a), the TEM images taken on the sample deposited on the grid from chloroform suspension showed much smaller (less than 50 nm) and very uniform particles (Figure 1d).

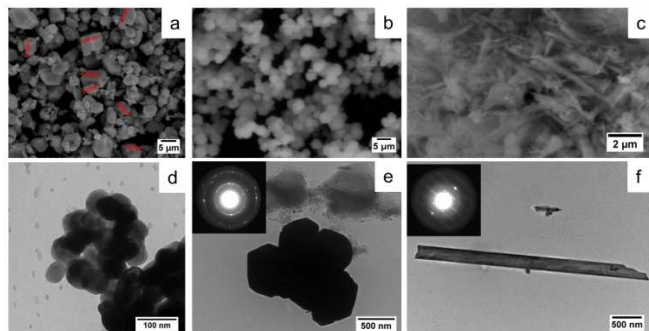


Fig. 1 Top - SEM images for: a - commercial barium titanate (CO); b - cubic barium titanate (CU); c - barium titanate nanorods (NR). Bottom - TEM images for: d - commercial barium titanate (CO); e - cubic barium titanate (CU); f - barium titanate nanorods (NR).

Each particle, as seen in TEM images, is composed of multiple crystalline grains, which in turn are composed of multiple crystallites. The sizes of the crystallites for the specific type of particles, calculated with Debye-Scherrer equation, are: 59 nm (CO), 58 nm (CU) and 60 nm (NR).

Wide angle X-ray powder diffraction spectra, registered at room temperature in the range 2θ from 20 – 70 ($^{\circ}$), show for both our samples (CU and NR) and for commercial sample (CO) the same patterns specific for crystalline barium titanate.³⁵ The presence of (100) planes shows that ferroelectric domains have 180° walls and act as boundaries between domains with antiparallel polarization and these form as a result of pressure developed in stainless steel autoclaves at 200°C.²¹

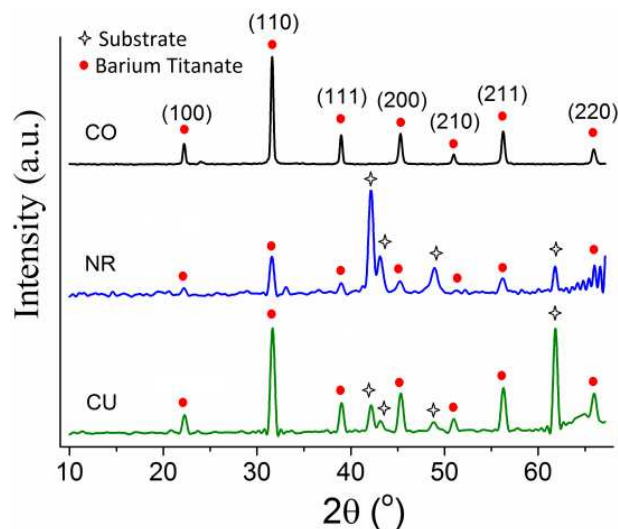
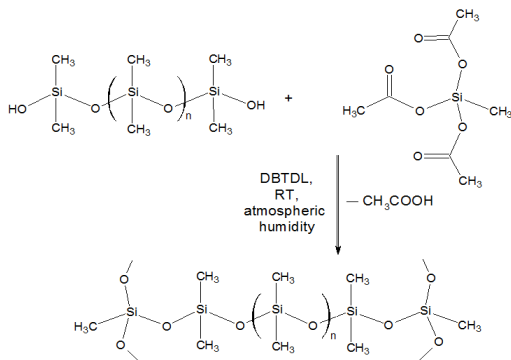


Fig. 2 X-ray powder diffraction spectra for barium titanate (BT) with cubic (CU) and nanorod (NR) morphologies in comparison with that of a commercial (CO) sample; assignment of diffraction peaks was made according to ref.³⁵

Using high concentration solutions of sodium hydroxide, contributes to increasing the concentration of the reaction mixture which favors the nucleation rate and the formation of smaller particles uniformly distributed. This is visible in Figure 2, where for cubic (CU) nanoparticles formed in 10M NaOH solution there is increased peak intensity of barium titanate.³⁶

Barium titanate species thus obtained were used as active fillers for PDMS. In order to assure a good compatibility of the filler with the matrix, the former was previously surface treated with a surfactant. A commercial surfactant, PLURONIC L-31 was used in this aim at a rate of 100 wt% relative to the mass of filler. Incorporation of the filler in the matrix was performed by mechanical stirring and sonication; the last operation was done in order to remove all the air bubbles trapped in the mixture.

The crosslinking occurred in films cast on the Teflon substrate by condensation using MTAS as a crosslinker agent and DBTDL as catalyst, in presence of the atmospheric moisture, at room temperature, according to Scheme 1.



Scheme 1 Crosslinking pathway applied for poly(dimethylsiloxane)- α,ω -diol matrix.

The distribution of the filler within the silicone matrix was emphasized by SEM images taken on cryofractured section (Figure 3). Contrary to expectations, the surfactant aggregates incorporating filler are visible as white particles, probably due to large amount of surfactant used (surfactant:filler = 1:1 weight ratio). However, the aggregates are relatively uniform distributed within the matrix. The stick morphology of the filler is observed in the case of the composite C-NR, where these were used (inset Fig 3b).

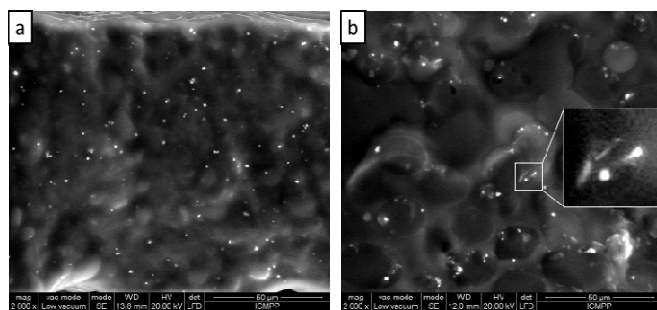


Fig. 3 SEM images in cryo-fractured section for the sample: a - C - CU; b - C - NR.

The impact of barium titanate particles, their size and morphology on some characteristics and properties of silicone composites thereof was studied by comparing the results with those obtained on a similar sample prepared without filler. Pure crosslinked PDMS shows very high value for the strain (2198 %) (Figure 4a, Table 1).

Table 1. The main parameters of the mechanical and dielectric tests.

Sample	Young's modulus ^a , MPa	Tensile strength, MPa	Elongation at break, %	Dielectric permittivity, ϵ' (at 10 Hz, 25°C)	Dielectric permittivity, ϵ' (at 5 kHz, 25°C)	Dielectric loss, ϵ'' (at 10 Hz, 25°C)	Ebf, ^b (kV/mm)	β , ^c MPa ⁻¹	τ^d (J)
C-R	0.0958	0.20	2198	3.11	3.01	0.21	102.28	31.42	6.37
C-CO	0.2330	0.17	1196	3.90	3.72	0.15	21.74	15.97	21.98
C-NR	0.0196	0.13	894	9.04	7.96	0.30	18.28	406.12	22.21
C-CU	0.1740	0.16	902	5.29	4.75	0.07	5.76	27.30	0.61

^aYoung's modulus calculated at 15% strain; ^bdielectric strength; ^celectromechanical sensitivity estimated according to ref.⁶ as a ratio between the dielectric permittivity at 5kHz and Young's modulus calculated at 15% strain; ^destimated energy output.⁴⁰

This is due to the high molecular mass of the used polymer. Being long and flexible, and because the crosslinking is achieved through the ends of the chain (giving freedom between crosslinking nodes), the polymeric chains are able to slide over each other in the absence of constraints imposed by other intermolecular forces. A decreasing of this value is observed as a result of incorporating the fillers, when the strain drops to about 900 % but this still is a good value compared with literature.^{13,14,37} This would be partially due to the plasticized effect of surfactant. The decrease of tensile strength and elongation in PDMS-BT composites proves the non-reinforcing effect of barium titanate as has also been found in another study.³⁷

Young's modulus increases as a result of the incorporation of prismatic barium titanate (commercial and cubic one), and this is an expected effect, according to the rule of mixtures. However, in the case of the composite filled with nanorods, Young's modulus decreases dramatically. We presume that the small dimensions of this filler, high dimensional ratio and good dispersion within matrix contribute to this result. In order to clarify this aspect further studies are needed.

Stress-strain cycles, with strains up to 100 % of initial length, show an viscoelastic behaviour (shown by stress relaxation, Figure 1ESI) in all cases with a clearly visible hysteresis loop only at the first strain-release cycle; in the subsequent strain cycles, the siloxane chains are rearranged in the film and the difference between strain and release was smaller than 1% of the stress value at each point (Figure 4b). In fact, this behavior might be associated with Mullins effect (first-cycles stress-softening³⁸), the temporary phenomenon which disappears after a few cycles of solicitation when the elastomer response is completely stabilized and reproducible as long as the maximum stretching level is not exceeded.^{38,39}

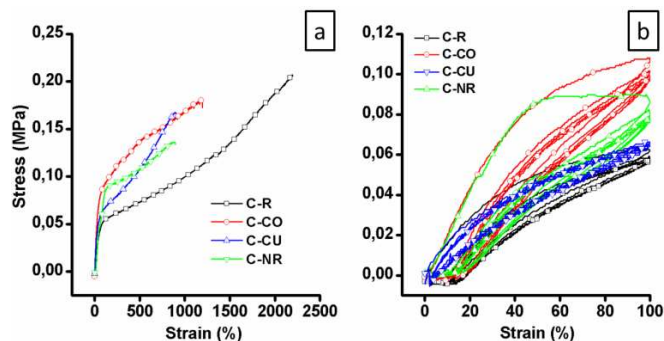


Fig. 4 Mechanical tests for the crosslinked films: a - stress-strain curves, b - mechanical fatigue behavior.

ARTICLE

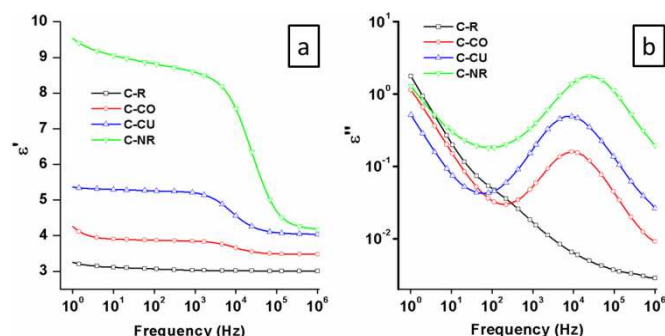


Fig. 5 Dielectric measurements for tested samples: a - dielectric constant; b - dielectric loss as a function of frequency.

Permanent set values (Figure 1ESI, Table 1ESI) reveal that the four samples have different elastic portions of the stress-strain curve. For sample C-R, the elastic portion is up to 20 %, with 0.01967 MPa of stress. A decreasing in the maximum limit of pure elastic strain at 10, 12.5 and 12.8 % occurs when commercial, nanorod and cubic barium titanate particles, respectively, are incorporated in the silicone elastomer while the stress values increase.

The dielectric behavior of the obtained composites is a normal one (Figure 5, Table 1). As expected, the dielectric permittivity of the silicone matrix increases by incorporation of barium titanate, a dielectric ceramic, the effect being more obvious when particles of filler have high aspect ratio, i.e., nanorods. Thus, while pure crosslinked PDMS have $\epsilon' = 3.01$ at 10 Hz, this increases at 3.90, 5.29 and around 8 by incorporating commercial barium titanate, prepared cubic and nanorods one, respectively. These values can be considered good if they are compared with those reported in the literature for some PDMS-BT composites that are close, for example $\epsilon' \sim 3.8$ (1Hz) at 5 wt% BT particles of 100 nm,⁴¹ or higher, $\epsilon' \sim 6.5$ ⁴² and $\epsilon' \sim 12$,³⁷ but obtained at a load of 20 vol% BT fibers⁴² or 30 php BT nanorods,³⁷ respectively. There is a sudden drop (the sharper as the value of the permittivity is greater) at about 10^4 Hz for ϵ' , accompanied with the maximum dielectric loss, ϵ'' , suggesting a relaxation process occurring at silicone-filler interface. The decrease in the dielectric permittivity is due to the inability of the dipoles, beyond a certain frequency, to orient and to return to the initial position in accord with the oscillating electric field. This happens when the time taken for the dipoles to return to its original random orientation, known as relaxation time, is larger than the rate of oscillating electric field. Thus, the polarization cannot follow the oscillating frequency resulting in the energy absorption and dissipation as heat.⁴²

For further applications as active elements in electromechanical actuation or energy harvesting devices, the dielectric parameters are very important besides the mechanical ones. The correlation of these two characteristic types is well expressed by electromechanical sensitivity, β , calculated according to established procedure⁶ as the ratio between the dielectric permittivity at 5 kHz and the Young's modulus at 15% strain (Table 1). The obtained value revealed that the morphology of the filler has a significant influence on this parameter. The highest effect proved to have the filler with high

aspect ratio - nanorods. By comparing the three composites containing the same percent of filler but with different morphologies, the sample C-NR shows an electromechanical sensitivity more than 12 times as that of pure PDMS. The three sensitivity values are higher as compared with other reported in literature for PDMS-BaTiO₃ composite for example⁶ (no information about the characteristics of the PDMS used as a matrix and applied crosslinking procedure has been provided).

As expected, the dielectric strength of the polymeric matrix consisting in crosslinked silicone fell when the filler has been incorporated into it (Table 1). However, values for samples C-CO and C-NR remain comparable with literature.^{1,13-15} On the basis of the measured dielectric strength values and elongation determined from mechanical tests, the energy gained from a stretching and relaxing uniaxial deformation cycle, τ (J), could be estimated according to literature.⁴⁰ While the energy output of the composite C-CU decreases dramatically (about 10 times) than the reference sample without any filler, C-R, the composite C-NR has shown a harvesting capacity more than three times higher (22.21 J) than sample C-R but only slightly higher than C-CO. The dielectric strength and higher value of elongation at break recorded for sample C-CO are those which contribute to raising it close to the energy output level recorded for sample C-NR, even if it has a lower dielectric constant.

For further applications, i.e., actuators, sensors or generators, the elastomer should also ensure a stable operation in different conditions of moisture and temperature.⁴³ The moisture sorption-desorption isotherms were registered in dynamic regime for the crosslinked composite films (Figure 6).

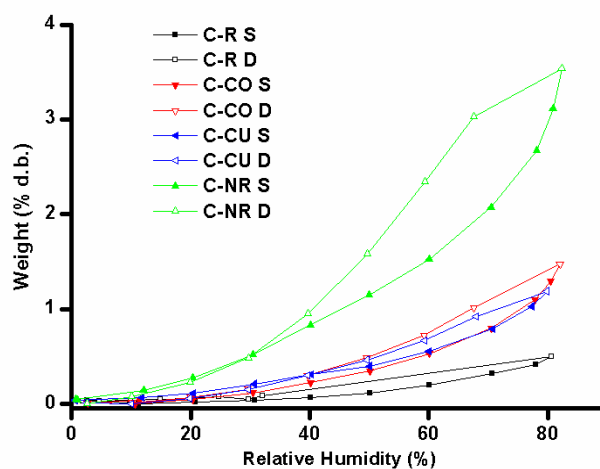


Fig. 6 Sorption-desorption isotherms of the reference sample C-R and composites C-CO, C-CU and C-NR registered at room temperature (the meaning of the endings: S - Sorption; D - Desorption).

Polydimethylsiloxanes and derived silicone materials are known as being very hydrophobic. An increase in moisture sorption capacity

of composites might have been expected due to the hydrophilic nature of the filler (barium titanate particles are easily dispersed in water). However, only a slight increase in the value of this characteristic was registered. Thus, the maximum sorption capacity increases from 0.50 % in pure crosslinked PDMS (C-R) to 1.18 % for the composite with cubic BT (C-CU), 1.47 % for the composite with commercial BT (C-CO) and 3.53 % in the composite with BT nanorods (C-NR). This diminished effect could be assigned to low loading filler level and the surfactant coating barium titanate particles combined with the known tendency of the polysiloxane to migrate at the interface material-air that will lead to a surface that is

richer in hydrophobic siloxane component. The higher value for the sorption capacity of the composite with BT nanorods as compared with the others could be explained by their higher specific surface. By their shape, isotherm recorded for the four samples could be associated with an isotherm of type III according to IUPAC classification – specific for non-porous hydrophobic materials with weak interactions between adsorbent-adsorbate. The kinetic curves (not shown) for water vapor sorption show the rate of desorption of water vapors are generally slower than the sorption rate, leading to a small hysteresis loop.

Table 2. Main centralized parameters obtained from TG/DTG and DSC data.

Sample	Stage ^a	T _{onset} ^b (°C)	T _{peak} ^c (°C)	T _{endset} ^d (°C)	Weight loss, %	Residue, wt% (700°C)	DSC data		
							T _g ^e	T _c ^f	T _m ^g
C-R	1	310.35	359.2	387.21	52.71	0.72	-121.5	-70.7	-38.16
	2	487.37	570	600.97	44.98				
C-CO	1	313.39	344	369.51	30.77	10.13	-120.6	-71.56	-39.16
	2	451.67	528.2 641.3	666.14	57.62				
C-NR	1	276.46	339.6	330.7	16.92	4.76	-124.2	-70.01	-42.39
	2	355.49	382.1	410.76	48.66				
	3	473.78	515.1	567.6	27.76				
C-CU	1	302.31	339	365.59	12.36	4.37	-120.61	-71.56	-39.16
	2	444.93	551.4	628.45	80.67				

^aStage of thermal degradation; ^bThe temperature at which the thermal degradation begins; ^cThe temperature at which the degradation rate reaches its maximum value; ^dThe temperature at which the process ends; ^eon the second heating run; ^fon the first cooling run.

Thermogravimetric analysis results (Figures 7, Table 2) reveal that both the reference samples and those filled with commercial and cubic barium titanate begin to decompose at 300-310 °C, the process occurring in two steps. Instead, the decomposition of the sample C-NR starts at 276 °C and occurs in three steps. Somewhat surprisingly, the reference sample is broken down almost entirely at 700 °C, the residue being 0.72 percent, although, according to silicon content, it would have been expected to be 81 %. We assume

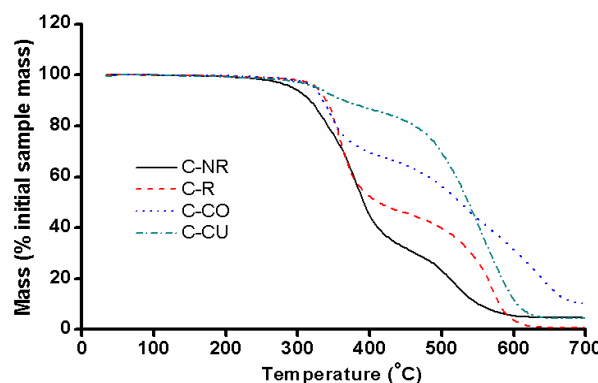


Fig. 7 Thermogravimetric curves registered for the prepared composites and reference sample.

that the presence in the sample of the dibutyltin dilaurate, used as crosslinking catalyst, causes the siloxane bond breaking which leads to the fragmentation of the long polysiloxane backbone turning it

into volatile compounds. The samples filled with barium titanate leaves higher residues due to the formation of metal oxides or ceramic materials. As can be seen from the data presented in Table 2, composite samples based on home-prepared barium titanate show similar values of thermal decomposition residues, 4.76 and 4.37 wt%, respectively, but lower than in the case of the sample containing commercial barium titanate that left a residue of 10.13 wt%. This difference may stem from the different preparation methods underlying the commercial and home-made barium titanate and different purity degrees. DSC analysis (Table 2) reveals that all the samples show transitions typical of silicone polymers: glass transition in the range -120 – (-140) °C, crystallization around -70 – (-71) °C and melting in the range -38 – (-42) °C without apparent modifications due to the presence of the filler. The peak corresponding to melting (at -40 °C) is smaller in area than the one corresponding for crystallization (at -70 °C) and this indicates that a small amount of crystalline phase develops during the cooling scan, due to the high degree of crosslinking. The DSC curves for the cooling scans overlap for the reference samples and the samples with barium titanate nanoparticles. However, the heating scans do not overlap, especially the sample with barium titanate nanorods C-NR, which shows an additional glass transition at -70 °C. This can be attributed to the surfactant which, as can be seen in the SEM image, in Figure 2b, is organized into larger aggregates in this case.

Conclusions

Barium titanate, with cubic and nanorod morphologies respectively, were obtained by hydrothermal procedure and then were incorporated in a high molecular weight polydimethylsiloxane matrix, followed by crosslinking. Very long chains and crosslinking system (through the ends of chains) used have created prerequisites for high elongations that actually have been acquired (between 894 and 2198 %). Incorporation of barium titanate into such an array resulted in composite materials with improved dielectric characteristics. The most effective was proven to be the filler having particles with high dimensional ratio (nanorods) which has led to a significant increase of dielectric permittivity of resulted composite (about three times) as compared with the matrix, the mechanical characteristics remaining in the domain of interest (Young modulus 0.0196 MPa and elongation around 900 %). The electromechanical sensitivity and gained energy capacity, parameters of interest for further target applications (active elements in electromechanical devices), estimated on the basis of the electrical and mechanical characteristics, proved to be 12 and more than three times higher, respectively for the composite filled with barium titanate nanorods than for pure crosslinked PDMS. These effects were obtained at lower load (5 wt%) than those reported in the literature for similar results. According to our knowledge, this is the first time when a PDMS having such high molecular weight is addressed in such purposes. All composites are stabilized after their first loading cycle. The moisture sorption and thermal stability of the PDMS changed to slightly increased values by the incorporation of the ceramic fillers, while the thermal phase transitions of the silicone matrix are almost unaffected by their presence.

Acknowledgements

The work presented in this paper is developed in the context of the project PolyWEC (www.polywec.org, prj. ref. 309139), a FET-Energy project that is partially funded by the 7th Framework Programme of European Community. Support by the COST Action (MP1003) "European Scientific Network for Artificial Muscles (ESNAM)", through Short-Term Scientific Mission COST-STSM-MP1003-14672, and PERCRO Laboratory -

TeCIP Institute - Scuola Superiore Sant'Anna Pisa Italy for technical support are also gratefully acknowledged. The authors addressed his thanks to Dr. V. Musteata, C. D. Varganici and F. Doroftei, for registration of dielectric spectra, thermal curves, and SEM images, respectively.

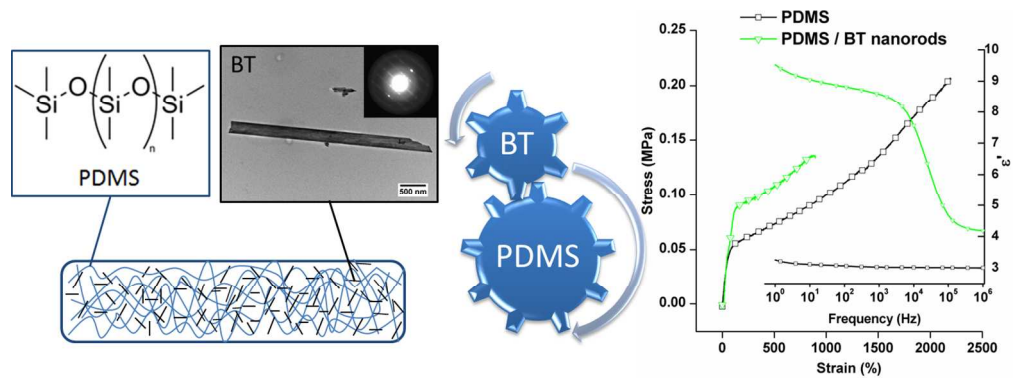
Notes and references

^a Petru Poni Institute of Macromolecular Chemistry, Aleea Grigore Ghica Voda 41A, Iasi, 700487, Romania. Fax: +40232211299;

Electronic Supplementary Information (ESI) available: Stress relaxation and permanent set data, DTG and DSC curves for the prepared composites. See DOI: 10.1039/b000000x/

- Z. Wang, J.K. Nelson, J. Miao, R.J. Linhardt, L.S. Schadler, H. Hillborg, S. Zhao, *IEEE Trans. Dielectr. Electr. Insul.*, 2012, **19**, 960-967 and references herein.
- B. Li, H. Chen, J. Zhou, *Compos. Part A: Appl. Sci. Manuf.*, 2013, **52**, 55-61.
- G. Kofod, H. Stoyanov, M. Kollosche, S. Risse, H. Ragusch, D.N. McCarthy, R. Waché, D. Rychkov, M. Dansachmüller. *Molecular level materials design for improvements of actuation properties of dielectric elastomer actuators. In: Proc. SPIE 7976, Electroactive Polymer Actuators and Devices (EPAD) 2011, 79760J*, March 2011. doi: [10.1117/12.880981](https://doi.org/10.1117/12.880981).
- S. Zhang, C. Zou, X. Zhou, D. Anderson, B. Zellers and Q. Zhang, *Polymer film capacitors with high dielectric constant, high capacitance density, and high energy density. In: Power Modulator and High Voltage Conference (IPMHVC)*, 2010 IEEE International, 2010 May 23-27; Atlanta, GA, pp. 221 – 224.
- X. Li, R. Zhang, W. Yu, K. Wang, J. Wei, D. Wu, A. Cao, Z. Li, Y. Cheng, Q. Zheng and R.S. Ruoff, *Zhu H. Sci. Rep.*, 2012, **2**, 870.
- H. Zhao, D.R. Wang, J.W. Zha, J. Zhao and Z.M. Dang, *J. Mater. Chem. A*, 2013, **1**, 3140-3145.
- G.M. Spinks, G.G. Wallace, L. Liu and D. Zhou, *Macromol. Symp.*, 2003, **192**, 161-170.
- P. Murugaraj, D. Mainwaring, N. Khelil, J.L. Peng, R. Siegele and P. Sawant, *Carbon*, 2010, **48**, 4230-4237.
- C. Naber, C. Tanase, P. Blom, G. Gelinck, A. Marsman, F. Touwlagel and S. Setayesh, *de Leeuw D. Nat. Mat.*, 2005, **4**, 243-248.
- R. Shankar, T.K. Ghosh and R.J. Spontak, *Soft Matter*, 2007, **3**, 1116–1129.
- S. Koulouridis, G. Kiziltas, Y. Zhou, D.J. Hansford and J.L. Volaki, *IEEE T Microw. Theory*, 2006, **54**, 4202–4208.
- M. Andriot, S.H. Chao, A. Colas, S. Cray, F. de Buyl, J.V. DeGroot, A. Dupont, T. Easton, J.L. Garaud, E. Gerlach, F. Gubbels, M. Jungk, S. Leadley, J.P. Lecomte, B. Lenoble, R. Meeks, A. Mountney, G. Shearer, S. Stassen, C. Stevens, X. Thomas and A.T. Wolf, *In Silicones in Industrial Applications*; F. Gubbels, R. De Jaeger, M. Gleria, Eds.; Nova Science Publishers: New York, 2007; 61-161.
- D.M. Opris, M. Molberg, C. Walder, Y.S. Ko, B. Fischer and FA. Nüesch, *Adv. Funct. Mater.*, 2011, **21**, 3531–3539.

14. S. Risse, B. Kussmaul, H. Krüger, R. Waché and G. Kofod, *DEA material enhancement with dipole grafting PDMS network*. In: Proc SPIE. 7976, *Electroactive Polymer Actuators and Devices (EAPAD)* 2011, 79760N. (March 24, 2011) doi: 10.1117/12.881919.
15. S. Risse, B. Kussmaul, H. Krüger and G. Kofod, *Adv. Funct. Mater.*, 2012, **22**, 3958-3962.
16. C. Racles, M. Cazacu, B. Fischer and D.M. Opris, *Smart Mater. Struct.* 2013, **22**, 104004 (10 pages).
17. S. Risse, B. Kussmaul, H. Krüger and G. Kofod, *RSC Adv.* 2012, **2**, 9029-9035.
18. J. Chon, S. Ye, K.J. Cha, S.C. Lee, Y.S. Koo, J.H. Jung and Y.K. Kwon, *Chem. Mater.*, 2010, **22**, 5445-5452.
19. Y. Rao, S. Ogitan, P. Kohl and C.P. Wong, *J. Appl. Polym. Sci.*, 2002, **83**, 1084-1090.
20. G. Subodh, V. Deepu, P. Mohanan and M. Sebastian, *Appl. Phys. Lett.*, 2009, **9**, 062903-062903.
21. L. Tu, A. Ilhan A. *Cryst. Growth Des.*, 2001, **1**(5), 401-419.
22. A. Sihvola and E. Alanen, *IEEE Trans. Geosci. Remot. Sens.*, 2002, **29**, 679-687.
23. Y. Bai, Z.Y. Cheng, V. Bharti and H. Xu, *Appl. Phys. Lett.*, 2000, **76**, 3804-3806.
24. K. Cheng, C.M. Lin, S.F. Wang, S.T. Lin and C.F. Yang, *Mater. Lett.*, 2007, **61**, 757-760.
25. S. Cho, J. Lee, J. Hyun and K. Paik, *Mater. Sci. Eng. B*, 2004, **110**, 233-239.
26. T. Hu, J. Juuti, H. Jantunen and T. Vilkmann, *J. Eur. Ceram. Soc.*, 2007, **27**, 3997-4001.
27. D. Khastgir and K. Adachi, *Polymer*, 2000, **41**, 6403-6413.
28. W.M. Winslow, *J. Appl. Phys.*, 1949, **20**, 1137-1140.
29. K. Koyama, K. Minagawa, T. Watanabe, Y. Kumakura and J. Takimoto, *J. Non-Newtonian Fluid Mech.*, 1995, **58**, 195-206.
30. K. Koyama, *Int. J. Mod. Phys. B*, 1996, **10**, 3067-3072.
31. L. Guo, H. Luo, J. Gao, L. Guo, and J. Yang, "Microwave hydrothermal synthesis of barium titanate powders," *Materials Letters*, vol. 60, no. 24, pp. 3011-3014, 2006.
32. M. Cazacu, M. Antohi, C. Racles, A. Vlad and N. Forna, *J. Compos. Mater.*, 2009, **43**, 2045-2055.
33. K.A. Andrianov, A.A. Zhdanov and A.A. Bogdanova, *Dokl. Akad. Nauk. SSSR*, 1954, **94**, 697-699.
34. Z. Lin, Y. Yang, J.M. Wu, Y. Liu, F. Zhang and Z.L. Wang, *J. Phys. Chem. Lett.*, 2012, **3**, 3599-3604.
35. Z. Lazarevic, N. Romcevic, M. Vijatovic, N. Paunovic, M. Romcevic, B. Stojanovic and Z.D. Mitrovic, *Acta Phys. Pol. A*, 2009, **115**, 808-810.
36. Shen Z., Zhang W., Chen J., Yun J., *Chinese J. Chem. Eng.*, 2006, **14**(5), 642-648.
37. A. Nayak, T.K. Chaki and D. Khastgir, *Adv. Mat. Res.*, 2013, **622-623**, 897-900.
38. L. Mullins, *Tubb. Chem. Technol.*, 1969, **42**, 339-362.
39. R. Vertechy, M. Fontana, G. Stiubianu and M. Cazacu, *Proc SPIE 9056, Electroactive Polymer Actuators and Devices (EAPAD) 2014*, 90561R (March 8, 2014); doi:10.1117/12.2045053.
40. S. Chiba, M. Waki, R. Kornbluh and R. Pelrine, *Smart Mater. Struct.*, 2011, **20**, 124006 (7pp).
41. A.L. Skov, A. Bejenariu, J. Bogelung, M. Benslimane and A.D. Egede, *Electroactive Polymer Actuators and Devices (EAPAD) 2012*, SPIE Vol. 8340, 83400M, 2012, doi: 10.1117/12.912114.
42. Z. Ahmad, *Polymer Dielectric Materials, Dielectric Material*, Silaghi MA (Ed.), ISBN: 978-953-51-0764-4, 2012, InTech, DOI: 10.5772/50638. Available from: <http://www.intechopen.com/books/dielectric-material/polymer-dielectric-materials>
43. E.A. Chigorina, T.M. Chigorina, A.A. Arutyunyan and M.V. Bestaev, *Polym. Sci. D*, 2010, **3**(4), 228-230.



Graphical Abstract
397x145mm (96 x 96 DPI)

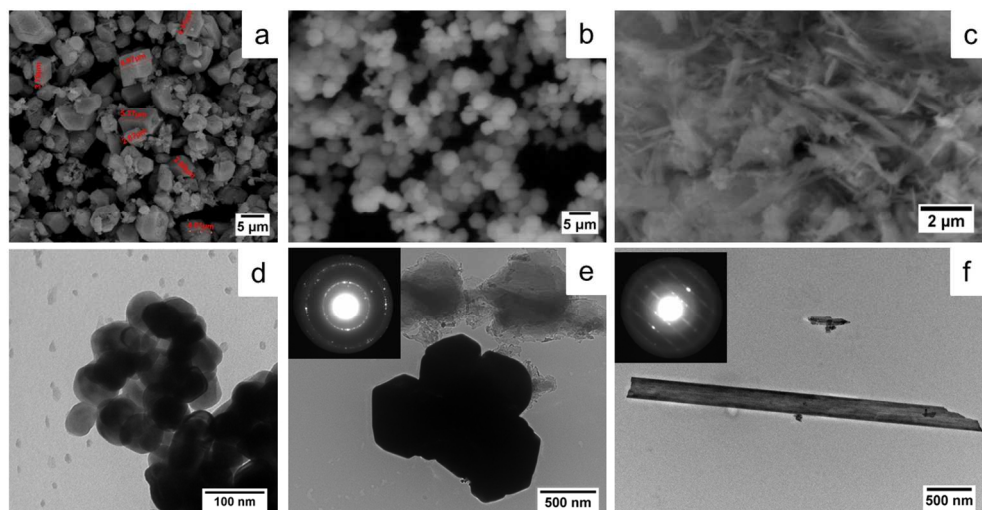


Fig. 1 Top - SEM images for: a - commercial barium titanate (CO); b - cubic barium titanate (CU); c - barium titanate nanorods (NR). Bottom - TEM images for: d - commercial barium titanate (CO); e - cubic barium titanate (CU); f - barium titanate nanorods (NR).
354x184mm (96 x 96 DPI)

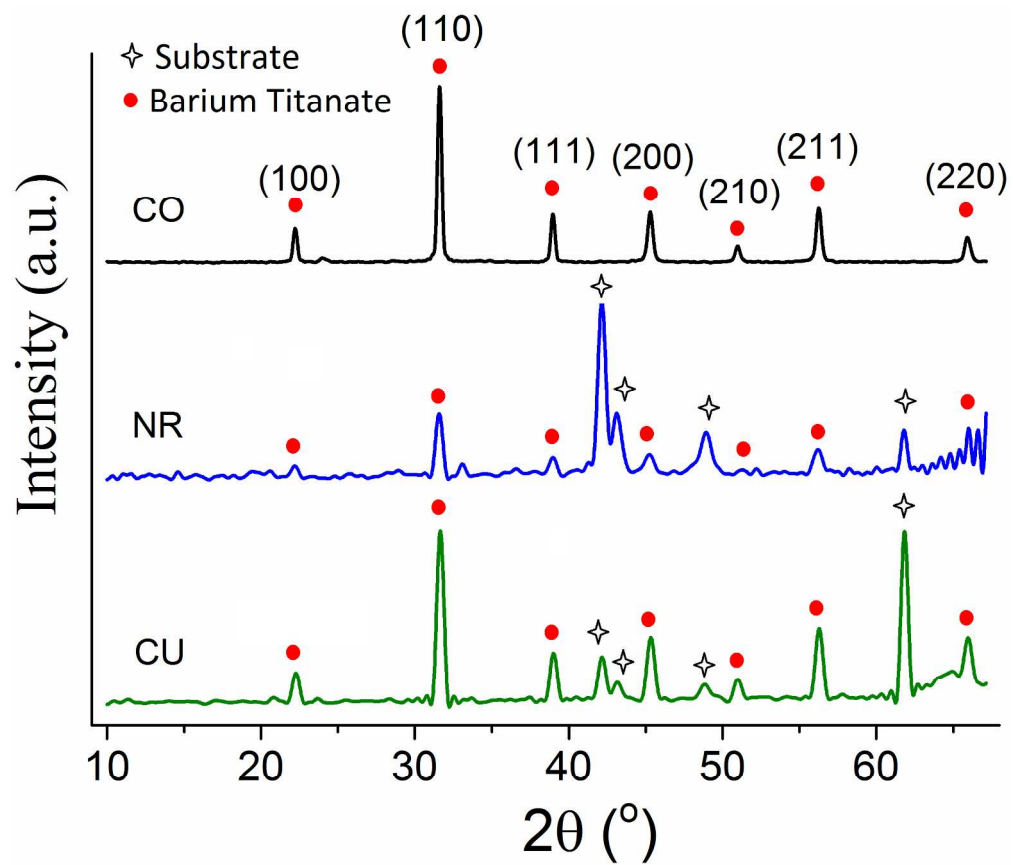


Fig. 2 X-ray powder diffraction spectra for barium titanate (BT) with cubic (CU) and nanorod (NR) morphologies in comparison with that of a commercial (CO) sample; assignment of diffraction peaks was made according to.35
217x187mm (300 x 300 DPI)

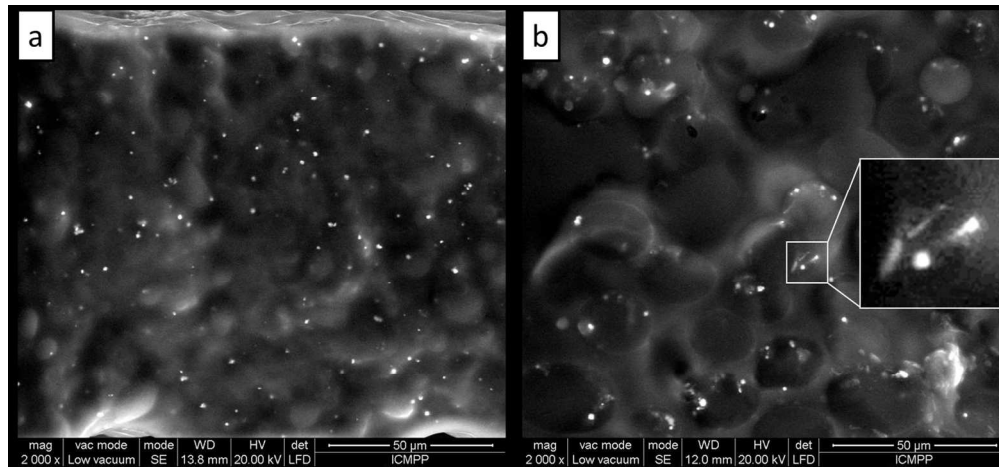


Fig. 3 SEM images in cryo-fractured section for the sample: a – C - CU; b – C - NR.
256x118mm (150 x 150 DPI)

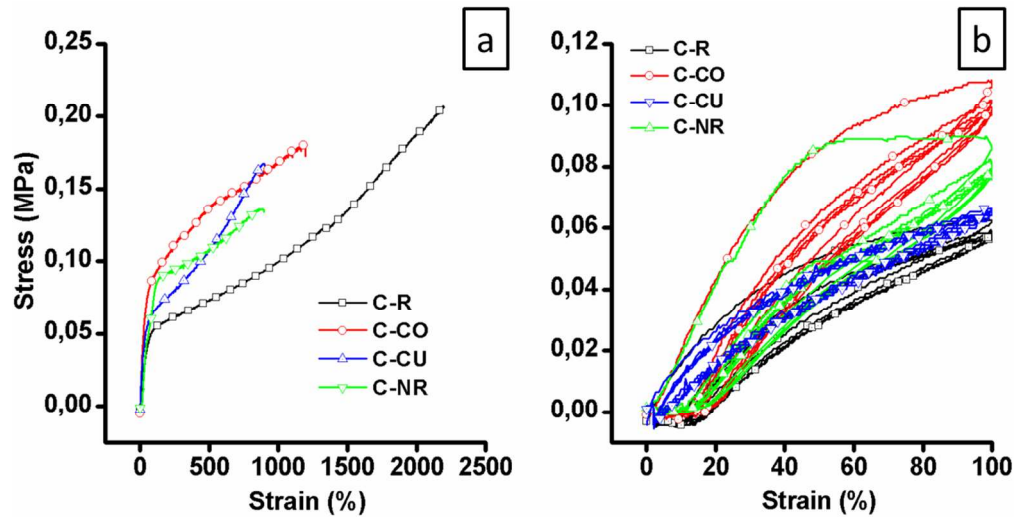
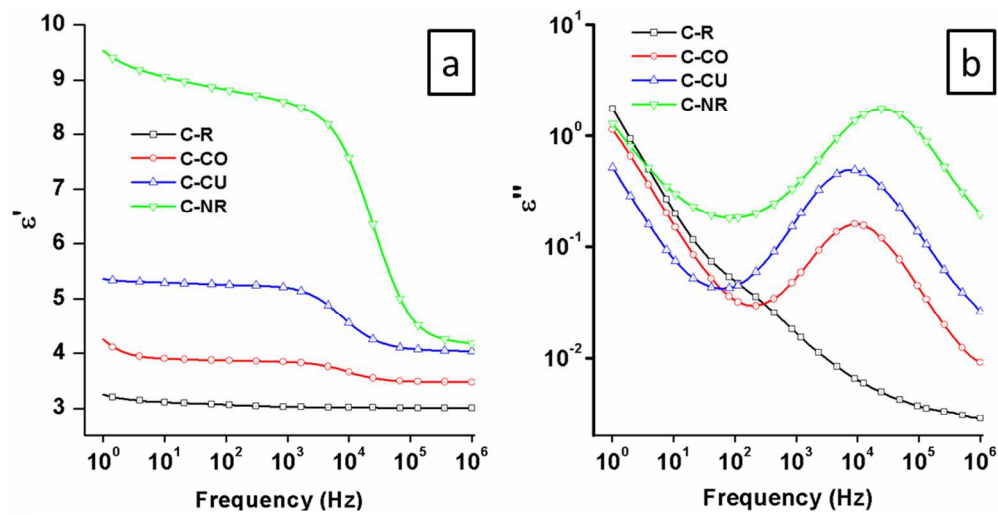


Fig. 4 Mechanical tests for the crosslinked films: a - stress-strain curves, b - mechanical fatigue behavior
332x171mm (96 x 96 DPI)



319x160mm (96 x 96 DPI)

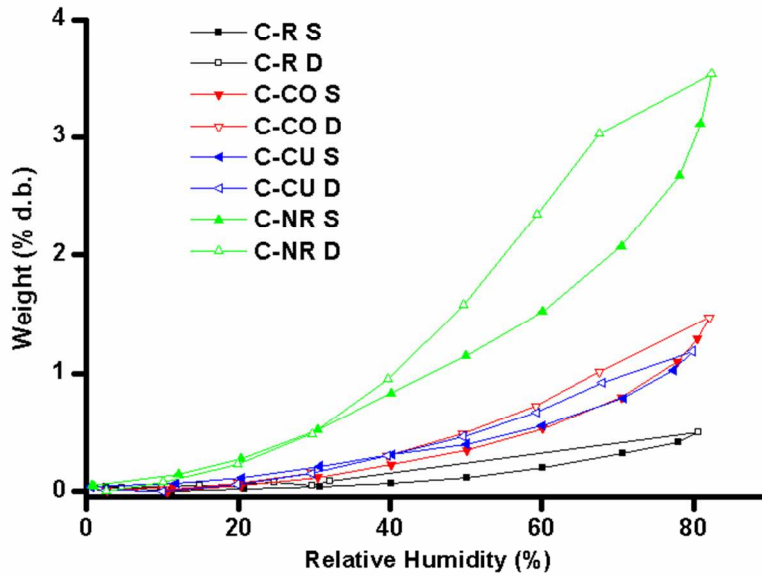


Fig. 6 Sorption-desorption isotherms of the reference sample C-R and composites C-CO, C-CU and C-NR registered at room temperature (the meaning of the endings: S - Sorption; D - Desorption)
76x50mm (300 x 300 DPI)

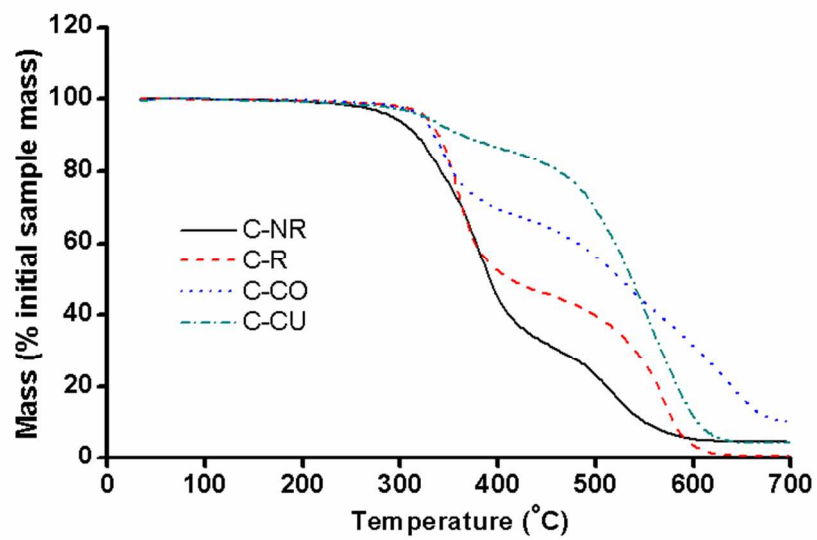


Fig. 7 Thermogravimetric curves registered for the prepared composites and reference sample.
76x45mm (300 x 300 DPI)

Supplementary information

Silicone-barium titanate composites with increased electromechanical sensitivity. The effects of the filler morphology

Adrian Bele, Maria Cazacu, George-Theodor Stiubianu, Stelian Vlad

“Petru Poni” Institute of Macromolecular Chemistry, Aleea Gr. Ghica Voda 41A, Iasi 700487,

Romania

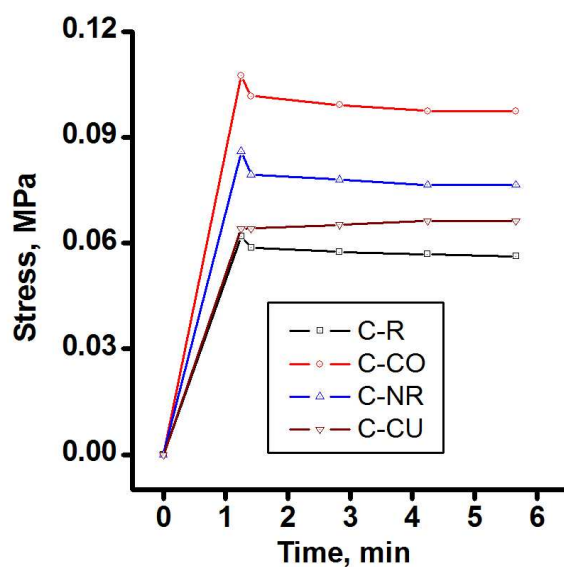


Figure 1ESI. Stress relaxation for tested samples

Table 1ESI. Permanent set for tested samples

Sample	Stress, MPa	Strain, %
C-R	0.01967	20
C-CO	0.02424	10
C-NR	0.02437	12.5
C-CU	0.03486	12.8

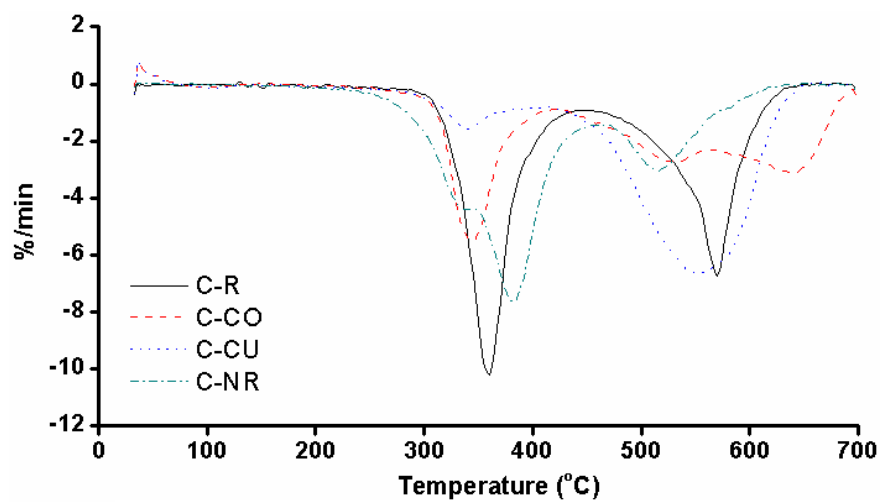


Figure 2ESI. DTG curves registered for the prepared composites and reference sample.

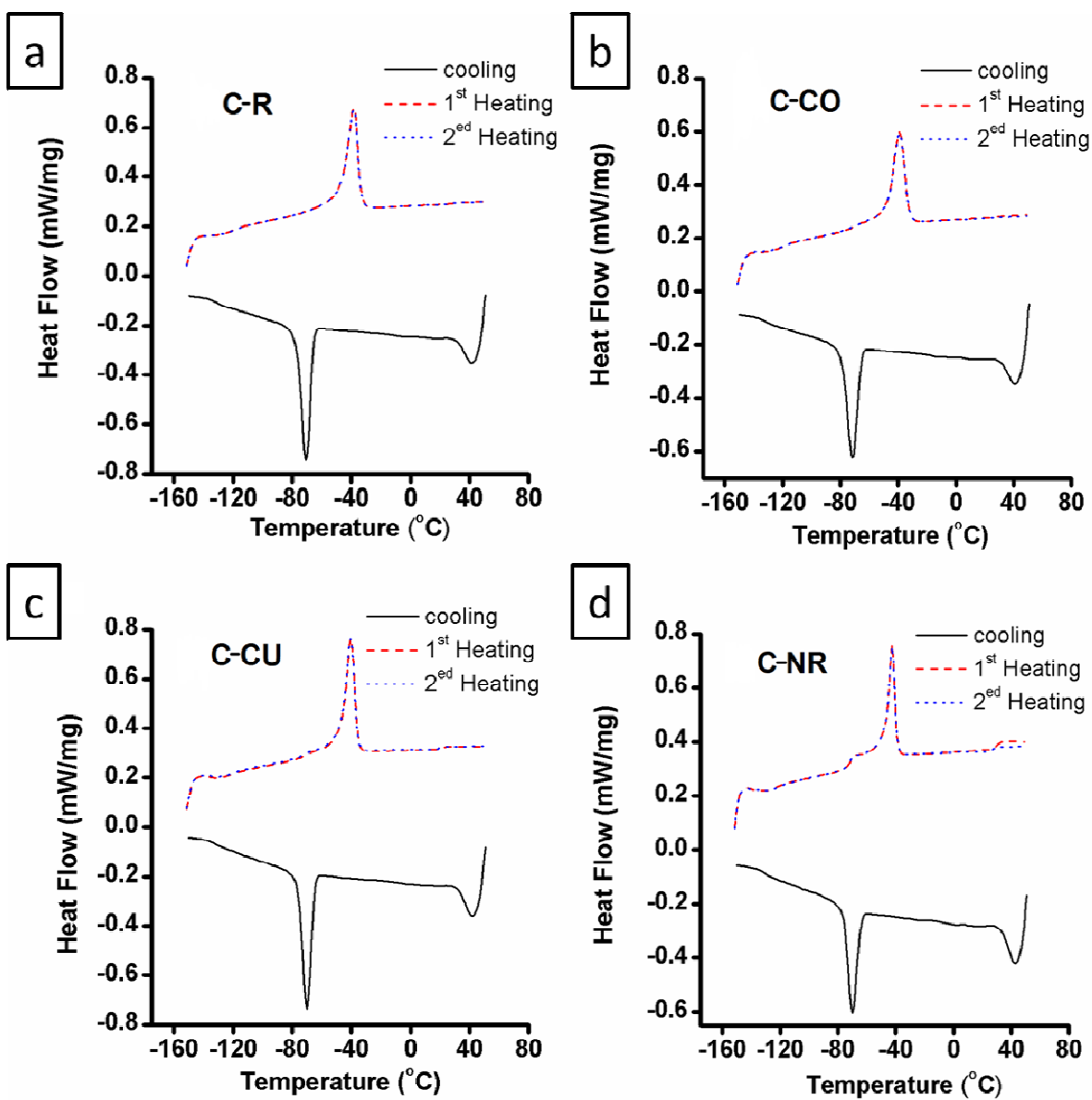


Figure 3ESI. DSC curves for the prepared composites as compared with reference sample.